Iopamidol: Exploring the Potential Use of a Well-Established X-Ray Contrast Agent for MRI

Silvio Aime,[3,4]* Luisella Calabi,[1] Luca Biondi,[1] Mario De Miranda,[1] Stefano Ghelli,[2] Lino Paleari,[1] Cristina Rebaudengo,[1] and Enzo Terreno[3,4]

Iopamidol is one of the most common contrast media used for diagnostic CT-based clinical protocols. Chemically, this molecule contains two pools of mobile protons (amide and alcoholic) that are in exchange with water. At 7.05 T, pH 7.4, and 312 K, the exchange rate of the alcoholic protons is too fast to affect the NMR properties of water protons, whereas the slowly exchanging amide protons induce a T_2-shortening effect on the "bulk" water signal that is detectable when the concentration is about 12 mM. Moreover, a more pronounced contrast is observed when the amide resonances are saturated by the application of an appropriate RF irradiation field, making iopamidol a potential chemical exchange saturation transfer (CEST) agent whose effect can be detected at a concentration as low as 7 mM (at 7.05 T). The exploitation of the MRI properties of iopamidol could facilitate novel and interesting diagnostic applications for combined MRI and CT studies. Magn Reson Med 53:830–834, 2005. © 2005 Wiley-Liss, Inc.

Key words: iopamidol; contrast agents; MRI; CEST; T_2 agent

Iopamidol has been used as diagnostic agent for clinical CT protocols since 1981. This nonionic contrast medium for X-ray imaging has very broad diagnostic applications, including disorders of the central nervous system, the cardiovascular apparatus, and the urinary tract (1–5).

The high water solubility shown by iopamidol, coupled with a very low toxicity, means that it can be safely administered intravenously at very high doses (up to 400 mg/ml).

In addition to the three iodine atoms necessary for endowing the system with high X-ray radiopacity, the chemical structure of iopamidol (chart 1) is characterized by the presence of three amide functionalities bearing hydrophilic substituents that are responsible for its outstanding water solubility.

Iopamidol possesses a high number of mobile protons (e.g., amide and alcoholic protons). We surmised that the occurrence of such a large pool of exchanging protons could be exploited as a source of contrast in an MR image. In fact, it is well established that proton exchange causes an increase in the water proton transverse relaxation rate (T_2 agent) (6–8), and may produce a more pronounced image contrast if the exchanging proton pool is irradiated with the appropriate radiofrequency (RF). This should lead to a decrease in the signal intensity of the water protons through the so-called chemical exchange saturation transfer (CEST) process (9). Both mechanisms contribute to a reduction in the MR signal intensity of the water protons, thus resulting in a darker spot in the MR image.

In this paper we report an in vitro study aimed at assessing the properties of iopamidol as a dual (T_2 and CEST) MRI contrast agent. In principle, if additional information can be gained from the MRI modality, one can envisage the potential clinical use of iopamidol in patients undergoing a CT exam.

MATERIALS AND METHODS

Iopamidol was kindly provided by Bracco Imaging, S.p.A (Milan, Italy).

NMR Measurements

All of the MR images were obtained on a Bruker Avance 300 WB spectrometer equipped with a microimaging probe head (Micro 2.5). The measurements were carried out on a phantom made of seven capillaries (~1 mm diameter) contained inside a 10-mm NMR tube filled with neat water. A 10-mm RF insert ($^1H/^{13}C$ inverse) was used. We measured T_1 using a multi-TR spin-echo sequence with TR values ranging from 0.25 to 8 s. T_2 was measured by means of a standard multiecho sequence with 24 TE values (5 ms step) starting from 5 ms.

We obtained CEST-MR images using a conventional spin-echo sequence (TE = 5 ms, TR = 20 s, one scan) preceded by a saturation pulse of variable length. The RF saturation offset was set at 1230 Hz (ν^{on}) or –1230 Hz (ν^{off}) with respect to the resonance of water protons. We obtained CEST difference images by subtracting the ν^{off} image from the corresponding ν^{on}one. The application of a train of sinc pulses (25 ms each, with an interpulse delay of 10 μs) provided the proper RF saturating field.

RESULTS AND DISCUSSION

We tested the ability of iopamidol to act as a dual contrast agent for MRI applications in vitro on a phantom (scheme 1) made of seven capillaries (1 mm in diameter) containing aqueous solutions of iopamidol at the following concentrations: 0, 13, 26, 65, 130, 260, and 520 mM.

Initially, a simple multi-TR spin-echo experiment was used to assess whether the presence of iopamidol could affect the longitudinal relaxation rate ($R_1 = 1/T_1$) of water protons. Figure 1a shows that R_1 is only slightly affected by the presence of the contrast agent.

[1]Bracco Imaging S.p.A., Centro Ricerche Milano, Milano, Italy.
[2]Spinlab, Rubiera, Italy.
[3]Dipartimento di Chimica IFM, Università di Torino, Torino, Italy.
[4]Molecular Imaging Center, Torino, Italy.
*Correspondence to: Silvio Aime, Dipartimento di Chimica IFM, Università di Torino, Via P. Giuria 7, 10125 Torino, Italy. E-mail: silvio.aime@unito.it
Received 20 April 2004; revised 10 November 2004; accepted 12 November 2004.
DOI 10.1002/mrm.20441
Published online in Wiley InterScience (www.interscience.wiley.com).

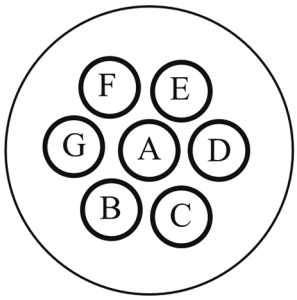

A = 0
B = 13 mM
C = 26 mM
D = 65 mM
E = 130 mM
F = 260 mM
G = 520 mM

Scheme 1.

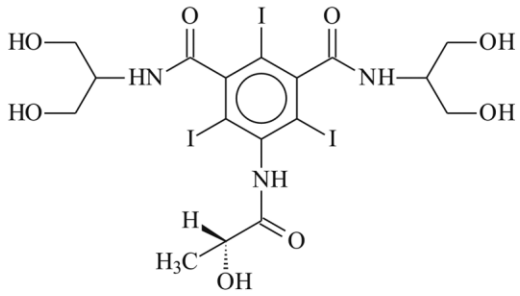

Chart 1

The concentration dependence of R_1 is linear (r = 0.992), with a slope (which may be considered as a sort of "longitudinal relaxivity" of the diamagnetic agent) of 5.2(± 0.3) · 10^{-4} $s^{-1}mM^{-1}$. The observed linear dependence between R_1 and iopamidol concentration probably reflects small changes in the viscosity of the solution. Clearly, iopamidol cannot be proposed as a T_1 contrast agent, since a positive contrast in the phantom image can only be detected for the solution of highest concentration (Fig. 1b).

As expected, this result simply shows that the R_1 values of water protons are not influenced by the chemical exchange with the mobile protons of iopamidol.

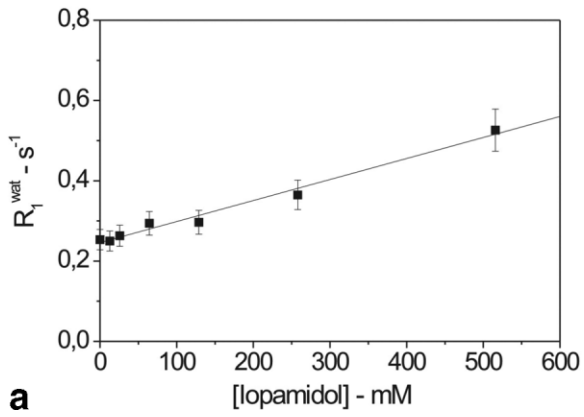

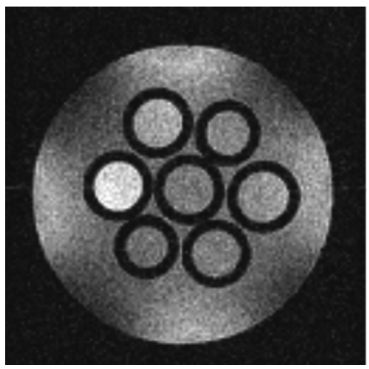

FIG. 1. **a:** Dependence of the longitudinal relaxation rate of water protons, R_1^{WAT}, on the iopamidol concentration (7.05 T, pH 7.4, 310 K). **b:** Spin-echo MR image of the phantom (TE = 3.4 ms, TR = 500 ms, 7.05 T, pH 7.4, 310 K).

Conversely, the proton exchange process significantly affects R_2 values. In fact, in a solution containing one major species *A* (e.g., water protons) in chemical exchange with a second species *B* (here represented by the mobile protons of iopamidol), the transverse relaxation rate of *A* can be adequately described by the Swift-Connick equation (10), which holds for any exchange regime and NMR window:

$$R_2^A = R_2^{A0} + p_M^B\, k_{ex}^B \left[\frac{R_2^B(R_2^B + k_{ex}^B) + \Delta\omega^2}{(R_2^B + k_{ex}^B)^2 + \Delta\omega^2} \right] \qquad [1]$$

where $R_2{}^{A0}$ is the transverse relaxation rate of *A* in the absence of *B*, $R_2{}^B$ is the transverse relaxation rate of *B*, k_{ex}^B is the pseudo first-order kinetic constant rate for the exchange of *B*, Δω is the chemical shift difference (in rad · Hz) between the two exchanging sites, and p_M^B is the molar fraction of *B*, i.e., $[B]/([B] + [A]) \approx [B]/[A]$.

Equation [1] clearly indicates that the influence of k_{ex}^B on $R_2{}^A$ is strictly dependent upon the values of $R_2{}^B$ and Δω.

Iopamidol contains both amide and alcoholic exchangeable protons (see chart 1). Usually, the exchange rate of the –OH protons in water is fast enough to satisfy the condition $k_{ex}^{OH} \gg \Delta\omega^{OH}$. As a consequence, it is not possible to observe the –OH absorptions in the high-resolution NMR spectrum of iopamidol under the experimental conditions used in this work (7.05 T, 310 K, and pH 7.4). Furthermore, for these protons, $k_{ex}^{OH} \gg R_2{}^{OH}$. Therefore, the presence of the mobile hydroxyl protons has a limited influence on $R_2{}^{wat}$, and Eq. [1] simply reduces to

$$R_2^{wat} \simeq R_2^{wat0} + \frac{p_M^{OH}\,\Delta\omega^2}{k_{ex}^{OH}} \qquad [2]$$

where the $(p_M^{OH}\Delta\omega^2)/k_{ex}^{OH}$ term is negligible owing to the small p_M^{OH} value and the occurrence of the $k_{ex}^{OH} \gg \Delta\omega^{OH}$ condition.

Conversely, the exchange regime of the amide protons is much slower, which allows their detection in the ^{1}H-NMR spectrum under the experimental conditions reported above. Consequently, for amide protons $\Delta\omega^{NH} \gg k_{ex}^{NH}$, although $R_2{}^{NH}$ still remains negligible with respect to k_{ex}^{NH}, with the exchange rate of the amide protons directly influencing $R_2{}^{wat}$. Now Eq. [1] can be written as

$$R_2^{wat} \simeq R_2^{wat0} + p_M^{NH}\, k_{ex}^{NH} \simeq R_2^{wat0} + \frac{n^{NH}[IOP]}{111.2} k_{ex}^{NH} \qquad [3]$$

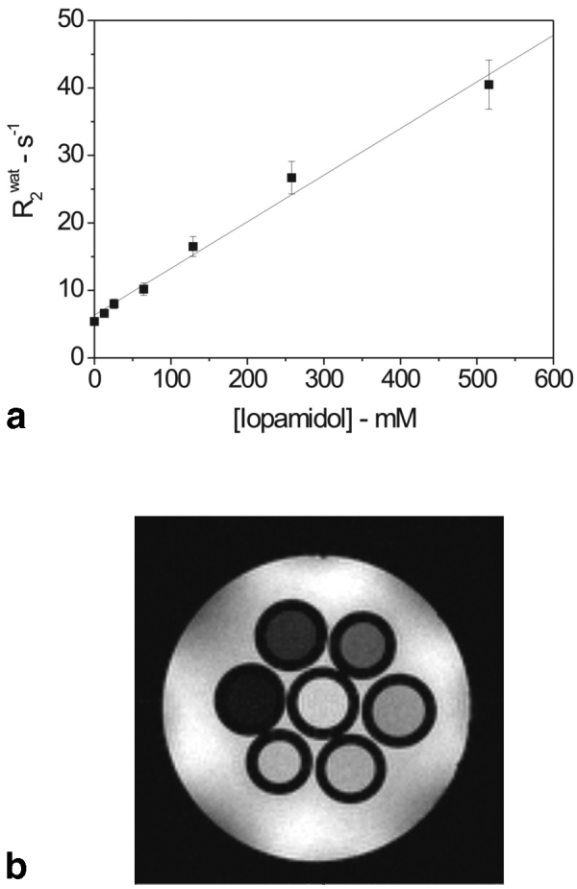

FIG. 2. **a:** Dependence of the transverse relaxation rate of water protons, R_2^{WAT}, on the iopamidol concentration (7.05 T, pH 7.4, 310 K). **b:** Spin-echo MR image of the phantom (TE = 120 ms, TR = 8000 ms, 7.05 T, pH 7.4, 310 K).

where n^{NH} refers to the number of amide protons per molecule, [*IOP*] is the molar concentration of iopamidol, and 111.2 is the molar concentration of water protons.

Figure 2a reports the R_2^{wat} values measured for solutions of the phantom using a conventional multiecho sequence. Similarly, in this case the concentration dependence is linear (r = 0.994); however, the slope is significantly steeper, resulting in a "transverse relaxivity" of 6.9 ($\pm$ 0.3) $\cdot$ 10^{-2} $s^{-1}mM^{-1}$ (i.e., 2 orders of magnitude larger than the corresponding longitudinal value).

Once the slope (i.e. the "transverse relaxivity") value is known, the exchange rate of the amide protons of iopamidol can be easily estimated using Eq. [3].

With the assumption that all of the amide protons of iopamidol have the same exchange rate, a k_{ex}^{NH} value of 2560 s^{-1} was obtained. This figure appears to be quite large for the exchange rate of an amide protons at pH 7.4 and 310K, but this result can be justified by the increased acidity of such protons due to the presence of the iodine atoms. A k_{ex}^{NH} value of 2560 s^{-1} confirms that at 7.05 T (proton Larmor frequency = 300 MHz, $\Delta\omega^{NH}$ = 7720 rad $\cdot$ Hz) the $\Delta\omega^{NH} > k_{ex}^{NH}$ condition is sufficiently satisfied ($(k_{ex}^{NH})^2$ is about 10% of $(\Delta\omega^{NH})^2$).

A typical MR image acquired in the multiecho type experiment (TE = 120 ms) is shown in Fig. 2b.

As expected, the solutions containing high amounts of iopamidol are markedly darkened, but it is still possible to detect a negative contrast of ~25% in the capillary containing the lowest concentration of contrast agent.

Interestingly, the fundamental requisite for enhancing R_2^{wat} through chemical exchange (i.e., $\Delta\omega > k_{ex}^{B}$) is also the basic requirement for a CEST-MRI agent. In fact, such agents are characterized by the presence of at least one set of mobile protons that upon irradiation contribute to a decrease in the signal intensity of water protons. This is brought about by the transfer of saturated magnetization, but only if the two exchanging sites are not in coalescence (9,11–16). The contrast-enhancing capability of CEST agents is usually evaluated in vitro by measuring the extent of the percent saturation transfer (ST%). This parameter is determined by performing two independent experiments differing in the irradiation frequency offset of the saturating RF pulse. In the first experiment the RF pulse is set to a frequency corresponding to the resonance of the mobile protons of the CEST agent (ν^{on}), and the resulting intensity of the water protons signal (resonating at $\nu = 0$) is I_S. In the second experiment, the saturating RF field is switched to a frequency $\nu^{off} = -\nu^{on}$, and the corresponding signal intensity of the water protons is I_0. The latter experiment is necessary to take into account any direct saturation effects on the water signal caused by the RF pulse. The ST% can be calculated using $[1 - (I_S/I_0)]$.

Because the ST efficiency is strongly affected by the irradiation frequency, we determined the most effective frequency offset corresponding by measuring ST% for a solution of iopamidol as a function of ν, and thus obtained the so-called *Z*-spectrum. The result (data not shown) led to an optimal frequency offset of 1230 Hz, which was used for all subsequent ST measurements.

Based on the assumption that the saturated magnetization of the amide protons of iopamidol is fully transferred to bulk water in the absence of residual direct saturation, the ST% obeys the following relationship, which is a rearrangement of an equation first described by Forsen and Hoffman (17):

$$ST\% = \left[1 - \left(\frac{I_s}{I_o}\right)\right]100 = \frac{k_{ex}^{NH}\, n^{NH}[IOP](1 - e^{-(111.2\, R_1^{irr} + k_{ex}^{NH}\, n[IOP]/111.2)t})100}{111.2R_1^{irr} + k_{ex}^{NH}\, n[IOP]} \quad [4]$$

where t is the irradiation time, and R_1^{irr}(equal to $1/T_1^{irr}$) is the longitudinal relaxation rate of water protons during irradiation of the mobile protons in the CEST agent. The correlation between R_1 and R_1^{irr} is not fully understood, although it is known that R_1^{irr} is larger than R_1 by a factor that is somehow dependent on k_{ex} (18). Equation [4] indicates that the extent of the ST is not dependent on the transverse relaxation rate of the bulk water protons. The analytical form of Eq. [4] is such that the ST% dependence on any of the involved parameters (k_{ex}^{NH}, n^{NH}, [*IOP*], and T_1^{irr}) is pseudohyperbolic and ST% tends to a plateau value.

This behavior is clearly displayed in Fig. 3, which indicates the influence of the irradiation time on ST% for the six iopamidol solutions of the above-described phantom.

It is interesting to note that the irradiation time at which the ST% reaches its maximum is inversely related to the

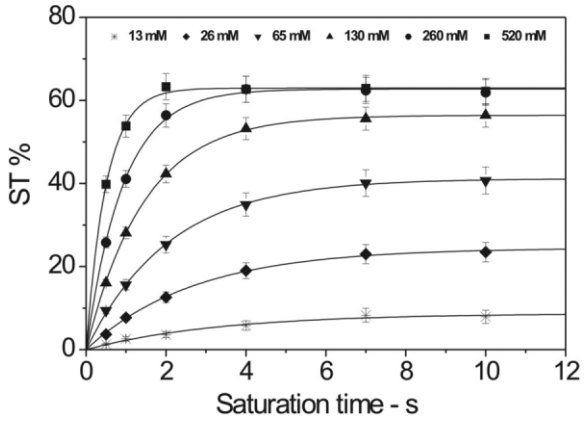

FIG. 3. Effect of the length of the saturating pulse on ST% (7.05 T, pH 7.4, 310 K). Irradiation of a train of sinc pulses 25 ms each (interpulse delay = 10 μs, irr. power = 4.65 μT) was applied. The data were fitted according to Eq. [6].

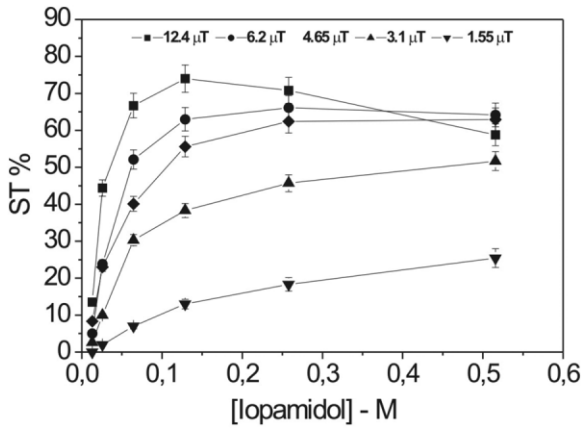

FIG. 4. Dependence of ST% on the concentration of iopamidol with varying saturation power (7.05 T, pH 7.4, 310 K, train of sinc pulses (25 ms each), interpulse delay = 10 μs, irradiation time = 7 s).

concentration of the CEST molecule. Since the *t*-value is crucial for determining the acquisition time of the MR images, we used a value of 7 s as a good compromise for the subsequent experiments.

We first analyzed the data represented in Fig. 3 using Eq. [4], keeping the values of n (3), [*IOP*], and k_{ex}^{NH} (2560 s^{-1}) fixed, but the obtained fittings were very poor. As already mentioned, Eq. [4] holds under the assumption that all the mobile spins of the CEST molecule are irradiated. Actually, the fraction of the saturated protons that are actually transferred, α_o^{NH}, is mainly dependent on k_{ex}^{NH} and the power of the saturating RF field (γB_1) (19):

$$\alpha_0^{NH} = \frac{(\gamma B_1/k_{ex}^{NH})^2}{1 + (\gamma B_1/k_{ex}^{NH})^2} \qquad [5]$$

Thus, we reanalyzed the data using the following equation:

$$\mathrm{ST\%} = \left[1 - \left(\frac{I_S}{I_0}\right)\right]100 = \frac{\alpha_0^{NH}\, k_{ex}^{NH}\, n^{NH}[IOP](1 - e^{-(111.2\, R_1^{irr} + \alpha_0\, K_{ex}^{NH}\, n[IOP]/111.2)t})100}{111.2\, R_1^{irr} + \alpha_0 k_{ex}^{NH}\, n[IOP]} \qquad [6]$$

This resulted in the excellent-fitting curves reported in Fig. 3. The values of the two parameters obtained from the fitting procedure, R_1^{irr} and α_o^{NH}, are listed in Table 1.

Table 1
R_1^{irr} and α_0^{NH} Values Obtained From the Analysis of the Data Shown in Fig. 3 using Eq. [6]

[IOP] (M)	R_1^{irr} (s^{-1})	α_0^{NHG}
0.013	0.27	0.030
0.026	0.28	0.050
0.065	0.28	0.045
0.13	0.3	0.044
0.26	0.4	0.038
0.52	0.74	0.035

The small R_1^{irr} enhancement that occurs when the concentration of iopamidol is increased is consistent with the view that the longitudinal relaxation rate of the water protons is not significantly affected by the concentration of iopamidol (see Fig. 1a), and, as mentioned above, the R_1^{irr} values are slightly larger than R_1.

Conversely, the α_o^{NH} values are not concentration-dependent; rather, these values indicate that only a small fraction of the mobile protons are actually saturated, thus contributing to the observed ST effect. The relatively low efficiency in the saturation of the amide protons of iopamidol is the result of a low-power saturation RF field compared to the exchange rate of the amide protons, i.e., $\gamma B_1 < k_{ex}^{NH}$.

This means that α_o^{NH} could be increased by the application of a higher-power saturation pulse. The dependence of the ST effect on the power of the saturation pulse is illustrated in Fig. 4. While it is clear that the ST efficiency is markedly affected by the power of the saturation pulse, it seems evident that the concentration of iopamidol is a relevant parameter.

In fact, although at concentrations lower than 0.1 M the ST% is directly proportional to the power of the saturation pulse, at higher concentrations this trend changes, and the ST% at 12.4 μT is smaller than the ST% at 4.65 μT for the 0.5 M solution. This finding is not particularly surprising, since increasing the power of the saturation pulse can lead to a broadening of the excitation bandwith, with a consequent direct saturation effect on the water proton signal. In this study, this effect was amplified because of the relatively small difference (only 1230 Hz) in the resonance frequency between the two exchanging sites. Nevertheless, the concentration dependence of ST% observed at the highest power level (12.4 μT) can not be theoretically justified. It is likely that the use of such a high-power pulse makes ST% dependent on the sample shimming. In fact, a nonperfectly Lorentzian signal can lead to a direct saturation effect that depends on the frequency offset (ν^{on} or ν^{off}) of the saturation pulse. Thus, the behavior shown in Fig. 4 could be explained by a larger direct saturation effect when the offset of the saturation pulse is positioned at ν^{off}.

Despite the problems associated with the use of a high-power saturation pulse, the train of sinc pulses with a

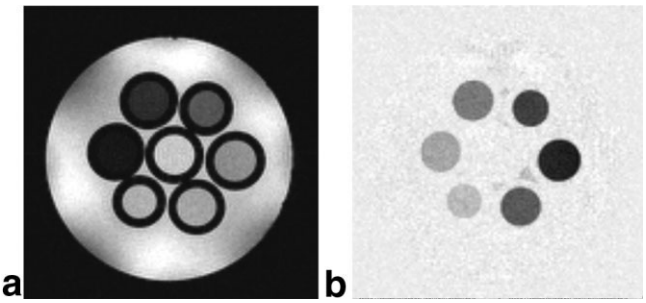

FIG. 5. Comparison between a T_{2w} MR image (on the left, also shown in Fig. 2b) and a CEST MRI difference (ν^{ON}-ν^{OFF}) image (on the right) of the same phantom (7.05 T, pH 7.4, 310K). (CEST MR images: train of sinc pulses (25 ms each), interpulse delay = 10 μs, irr. time = 7 s, irr. power = 12.4 μT).

power of 12.4 μT ensures an efficient ST for iopamidol concentrations lower than 0.1 M.

The body of data collected so far on the phantom containing iopamidol clearly indicates that this molecule can act as either a T_2- or a CEST-MRI contrast agent. On this basis, it is of interest to ascertain the minimum concentration of iopamidol required to detect a contrast in the two imaging modalities.

Figure 5 shows a comparison of two MR images of the same phantom. On the left is the spin-echo T_{2w} image shown in Fig. 2b, whereas on the right a CEST difference image obtained by subtracting the ν^{off} image from the corresponding ν^{on} (saturation power 12.4 μT, irradiation time 7 s) is shown. Let us focus on the contrast between capillaries A and B, which contain pure water, and a 13-mM solution of iopamidol, respectively. It is evident that the contrast is definitely better in the CEST difference image, probably because the image difference cancels out the signal of the water protons in the regions in which there is no ST effect. This explanation may justify why the minimum ST% value for detecting contrast is approximately 5%, whereas in T_{2w} images the requested signal difference has to be about 25%. On this basis, the sensitivity of iopamidol as CEST agent is definitely higher (minimum amount = ~7 mM, saturation power = 12.4 μT, irradiation time = 7 s) than that estimated if the same molecule acts as a T_2 agent (minimum amount = ~12 mM).

The higher sensitivity shown by the CEST modality vs. the T_{2w} images is balanced by some drawbacks. For instance, the CEST technique is much more time-consuming because it requires the saturation of the mobile protons and the acquisition of two images. Another possible drawback in vivo may arise from the presence of mobile protons belonging to endogenous molecules whose resonance frequency can overlap with the absorption region of iopamidol amide protons. Therefore, the ST% value could be either over- or underestimated.

CONCLUSIONS

The results obtained in this work indicate that iopamidol, one of the most commonly used contrast agents for CT, may be also considered as a contrast medium for MRI applications. In fact, the presence of a pool of amide protons in relatively slow exchange with the bulk water protons can considerably reduce the signal intensity in an MRI experiment through two distinct modalities: R_2 enhancement and CEST. The combined use of both techniques may be of interest for some specific clinical applications.

ACKNOWLEDGMENT

We thank Mr. Paul Atkinson for improving the language in the manuscript.

REFERENCES

1. Pitrè D, Felder E. Development, chemistry and physical properties of iopamidol and its analogues. Invest Radiol 1980;15:301–309.
2. McKinstry DN, Rommel AJ, Sugerman AA. Pharmacokinetics, metabolism and excretion of iopamidol in healthy subjects. Invest Radiol 1984;19:171–174.
3. Dawson P, Bradshaw A, Hill C. Jopamiron: a new non-ionic contrast medium. Acta Radiol Diagn 1984;25:253–256.
4. Mutzel W, Speck U. Tolerance and biochemical pharmacology of Jopamiron. Rofo 1983;118–125.
5. Bourin M, Jolliet P, Ballereau F. An overview of the clinical pharmacokinetics of x-ray contrast media. Clin Pharmacokinet 1997;32:180–193.
6. Aime S, Nano R, Grandi M. A new class of contrast agents for magnetic resonance imaging based on selective reduction of water-T_2 by chemical exchange. Invest Radiol 1888;23(Suppl 1):S267–S270.
7. Aime S, Botta M, Barbero L, Uggeri F, Fedeli F. Water signal suppression by T2-relaxation enhancement promoted by dysprosium(III) complexes. Magn Reson Chem 1991;29:S85–S88.
8. Muller RN, Bulte JVM, Gillis P, Roch A, Laurent S, Botteman F, Vander Elst L. Impact of water exchange kinetics on the transverse relaxivity of some Dy-DTPA derivatives, potential negative contrast agents for high field imaging. MAGMA 1999;8:S13–S14.
9. Ward KM, Aletras AH, Balaban RS. A new class of contrast agents for MRI based on proton chemical exchange dependent saturation transfer (CEST). J Magn Reson 2000;143:79–87.
10. Swift TJ, Connick RE. NMR-relaxation mechanism of O-17 in aqueous solutions of paramagnetic cations and the lifetime of water molecules in the first coordination sphere. J Chem Phys 1962;37:307.
11. Goffeney N, Bulte JVM, Duyn J, Bryant Jr LH, van Zijl PCM. Sensitive NMR detection of cationic-polymer-based gene delivery systems using saturation transfer via proton exchange. J Am Chem Soc 2001;123:8628–8629.
12. Zhang S, Michaudet L, Burgess S, Sherry AD. The amide protons of a ytterbium(III)-DOTA-tetraamide complex act as efficient antennae for transfer of magnetization to bulk water. Angew Chem Int Ed 2002;41:1919–1921.
13. Aime S, Delli Castelli D, Terreno E. Novel pH-reporter MRI contrast agents. Angew Chem Int Ed 2002;41:4334–4336.
14. Zhang S, Merritt M, Woessner DE. PARACEST agents: modulating MRI contrast via water proton exchange. Acc Chem Res 2003;36:783–790.
15. Aime S, Delli Castelli D, Terreno E. Supramolecular adducts between poly-L-arginine and Tm(III)DOTP: a route to sensitivity enhanced MRI-CEST contrast agents. Angew Chem Int Ed 2003;42:4527–4529.
16. Terreno E, Delli Castelli D, Cravotto G, Milone L, Aime S. Ln(III)-DOTAMGly complexes: a versatile series to assess the determinants of the efficacy of paramagnetic chemical exchange saturation transfer agents for magnetic resonance imaging applications. Invest Radiol 2004;39:235–243.
17. Forsen S, Hoffman RA. Study of the moderately rapid chemical exchange reactions by means of nuclear magnetic double resonance. J Chem Phys 1963;39:2892–2901.
18. Kruiskamp MJ, van Vliet G, Nicolay K. ^{1}H and ^{31}P magnetization transfer studies of hindleg muscle in wild-type and creatine kinase-deficient mice. Magn Reson Med 2000;43:657–664.
19. Snoussi K, Bulte JWM, Guéron M, van Zijl PCM. Sensitive CEST agents based on nucleic acid imino proton exchange: detection of poly(rU) and of a dendrimer-poly(rU) model for nucleic acid delivery and pharmacology. Magn Reson Med 2003;49:998–1005.